International Journal of Early Childhood Special Education (INT-JECSE)
DOI:10.9756/INTJECSE/V14I5.249 ISSN: 1308-5581 Vol 14, Issue 05 2022

Enhancing Segmentation Approaches from Super Pixel Division Algorithm to Hidden Markov Random Fields with Expectation Maximization (HMRF-EM)

Christo Ananth,
Department of Natural and Exact Sciences, Samarkand State University, Uzbekistan.

S. Amutha*,*
Assistant Professor, SCOPE, VIT Chennai, India.

K. Niha,
Assistant Professor, SCOPE, VIT Vellore, India.

Djabbarov Botirjon Begimovich, Basic Doctoral Student, Samarkand State University, Uzbekistan.

Abstract--- In surgical planning and cancer treatment, it is crucial to segment and measure a liver tumor's volume accurately. Because it would involve automation, standardisation, and the incorporation of complete volumetric information, accurate automatic liver tumor segmentation would substantially affect the processes for therapy planning and follow-up reporting. Based on the Hidden Markov random field, Automatic liver tumor detection in CT scans is possible using hidden Markov random fields (HMRF-EM). A CT scan of the liver may be too low-resolution for this software. CT liver tissue segmentation is based on the HMRF model. When building an accurate HMRF model, an accurate initial image estimate is crucial. Adaptive K-means clustering is often used for initial estimation. HMRF's performance can be greatly improved by clustering. This project aims to segment liver tissue quickly. This paper proposes an adaptive K-means clustering approach for estimating liver images in the HMRF-EM model. The previous strategy had flaws, so this one fixed them. We compare the current and proposed methods. The proposed method outperforms the currently used method.

Keywords--- Hidden Markov Random Field, CT Scan, Adaptive K Means.

I. Introduction

The complicated nature of medical image segmentation can be attributed to the absence of clearly defined tissue boundaries and artifacts produced by the neurological structure. In 2015, reports compiled by the World Health Organization placed liver cancer in the world's second leading cause of death due to cancer. The most prevalent form of primary liver cancer is hepatocellular carcinoma (HCC), ranked number six on the overall list of cancers [1]. In addition to this, it is not unheard of for a second tumour to develop in the liver at some point in time. The processes that are involved in the planning of liver therapy might benefit from the accurate and rapid segmentation of lesions, which would allow for the subsequent determination of volume- and texture-based information. This would allow for the segmentation of lesions to be performed more quickly. This would be feasible as a result of improvements in the accuracy with which

lesions could be localized. In addition to this, the utilization of a method of segmentation that is both standardised and automatic would result in a more reliable therapeutic response [2]. The size, appearance, and location of liver tumors can vary quite a bit from one patient to the next, as can the shape and appearance of the tumor. Depending on the healthy liver parenchyma that is surrounding them, they may appear hyperdense (brighter) or hypodense (darker) [3]. They may have a rim as a result of the accumulation of contrast agent, calcification, or necrosis, and they may appear either darker or brighter than the healthy liver parenchyma that is surrounding them. This is due to the fact that they contrast with the healthy liver parenchyma. It is possible for there to be a significant difference in the appearance of the lesion depending on factors such as the type of lesion, its state, the imaging (equipment, settings, contrast method, and timing), and the patient. Additionally, it is possible for there to be a significant difference in the appearance of the lesion. In addition to this, the appearance of the lesion may be quite different from one instance to the next. Because of the high degree of variability among liver lesions, sometimes it can be difficult to segment liver lesions in clinical settings. This is because liver lesions vary so much. The process of segmenting liver tumours has a wide variety of applications, some of which include the planning and evaluation of treatments, and it is necessary to decide which therapies to use.

However, manually outlining the boundaries of a tumor is a complex process that takes a lot of time and has the potential to be inaccurate at times. Because of this, there is a growing interest in image segmentation methods that are derived from appropriate medical imaging modalities. This is a direct consequence of the previous point. Several published pieces of medical research have presented various segmentation strategies for liver tumors on computed tomography (CT) images. These strategies have been suggested for use. Statistical analysis-based techniques include, among others, those that are watershed-based [4], deformable models such as active contours [5, 6], level set [7, 8], region growing technique [9, 10], voxel classification [11, 12], adaptive thresholding, and morphological processing techniques [13]. Watershed-based techniques can be found here. The vast majority of these methods do not make use of the information that is provided by the voxel's neighbourhood, which can result in an inaccurate segmentation of the liver's surface. This is especially the case when large tumors are present in the body. In addition to this, they demand a considerable investment of one's time and memory. Specific techniques, such as clustering, region growing, and thresholding, are utilised quite frequently in the process of medical image segmentation. This is because these techniques require a relatively small amount of computational resources and are simple to put into practice. The fact that these methods do not make use of the data on the intensity of the light is, however, the most significant drawback associated with them. Consequently, these techniques are vulnerable to boundary leakage when applied to tumors with fuzzy borders. Because of this, prior knowledge or other algorithms were incorporated [14, 15, 18] in order to lower the risk of either under-or over-segmentation.

II. Related Work

In their paper [14], Anter and colleagues presented a method for the automatic segmentation of tumors. The method relies primarily on a tool known as adaptive region growth to accomplish its objectives. With the assistance of a piece of software known as the marker-controlled watershed algorithm, the starting seed points for the region's expansion were figured out. This algorithm was utilised to assist in locating the initial seed points that were used. Zhou et al. [15] presented the findings of a study in which they compared and contrasted the performance of

three different semiautomatic approaches to the process of segmenting tumors. This study was conducted so that the researchers could better understand which method performed the best. These strategies include 2D knowledge-based constraints and 3D Bayesian rule-based region growing. Kumar et al. [16] developed CAD to segment and classify tumours. It's also abbreviated. This method is also called CAD. During segmentation, a new fuzzy clustering algorithm was used. This algorithm's success may be due to its non-Euclidean distance function. This is a proposed explanation. Adaptive thresholding, morphological processing, and a kernelized fuzzy C-means (FCM) algorithm helped Das and Sabut et al. [18] segment liver tumours from CT images. This method worked. Moghbel et al. [17] proposed a supervised random walker-based algorithm for tumour segmentation. This algorithm automatically divided tumours. FCM combined with cuckoo optimization was used to label pixels before the random walker segmentation was finished. Among the many different kinds of segmentation techniques, active contour approaches are among the most common. The level set algorithm and the fast marching algorithm are two of the most common segmentation techniques, and both of these algorithms fall under this category. However, to get accurate results from the segmentation process, you need to have good initialization functions and good speed functions. This is especially true for tumors with varying intensities and boundaries that are not very strong, as both are common in cancerous growths. In particular, this holds true for tumors that have both of these characteristics. This is because cancerous growths typically spread. The new level set model proposed by Li et al. [19] takes into account historical data, but it also takes into account information that is edge- and region-based. The FCM algorithm was used in order to generate a probabilistic estimation of the tumour tissues. This was done in order to understand the disease better. In the study that was conducted by Le et al. [20], the researchers came up with a method that is capable of semiautomatically segmenting liver tumors from Magnetic Resonance (MR) images.

The labelled regions in this method were produced with the help of the fast marching algorithm, and the unlabeled voxels that were still present after the initial round of labelling were categorized with the help of a neural network. This method was used to determine how to utilize this method best. Graph cuts methods are also utilised quite extensively for the purpose of medical image segmentation [22]. For the purposes at hand, these methods are an excellent choice due to their ability to produce an optimal solution globally. Stawiaski et al. [21] described an interactive segmentation method they had proposed in their work. This data segmentation technique was based on watershed and graph cuts. Semiautomatic and automatic methods competed against each other in the 2008 Liver Tumor Segmentation Challenge (LTSC08), which was held at the Medical Image Computing and Computer-Assisted Intervention (MICCAI) 2008 conference. The competition was held in conjunction with the Medical Image Computing and Computer-Assisted Intervention conference. This objective was successfully completed due to the method's success in achieving the highest level of accuracy possible among automatic approaches. Linguraru et al. [22] presented an automatic method for the segmentation of tumors in their study. [citation needed] When it comes to the target type of tumor that needs to be segmented, this method segments blob-like tumors more effectively than other types. This technique uses shape constraints derived from Hessian and is founded primarily on graph cuts as its underlying structure. Methods that are based on level sets or graph cuts, on the other hand, have the disadvantage of requiring a relatively high amount of computation, which is especially problematic for three-dimensional volume data. This problem can be avoided by using a method that is not based on level sets or graph cuts. This is the most significant disadvantage of both of

these different kinds of approaches. This is the situation because both graph cuts and level sets involve a significant amount of complexity. Researchers have also investigated techniques that are based on machine learning in order to account for variations in tumor size, shape, intensity, and texture. This was done in order to diagnose cancer better. This was done to ensure that the results are as accurate as possible. In the study that Foruzan conducted and Chen et al. [28], the support vector machine (SVM) was combined with the algorithm for approximating scattered data to locate the tumor's initial boundary. Following that, a sigmoid edge model was utilized in order to achieve a higher level of accuracy in the final lesion region. Kadoury et al. [24] developed a framework for the automatic segmentation of tumors by making use of a machine learning technique that was based on discriminant Grassmannian manifolds. Because of this, the tumors were able to be segmented in an accurate and productive manner. Because of this, tumors were able to be segmented automatically in an accurate and timely manner. Because of this, the tumours were able to be cut away from the surrounding tissue in a manner that was not only accurate but also efficient in terms of both time and effort. During the training phase of the procedure, the nonlinear intensity distributions of both liver and tumor tissues were studied and internalized as factual information. In order to section the tumor, a conditional random field (CRF) method of a higher order was utilised. The author's Zhang et al. [23] segmented the tumors by first applying a watershed transform to the liver region and then classifying them utilizing a region-based support vector machine. This process was repeated until the tumours were properly categorized. This was done in order to figure out where the tumours were located throughout the body.

Methods based on machine learning, on the other hand, require a significant amount of training data and gold standards to train correctly. Our goal was to develop a method for segmenting tumors that was quick, accurate, and reliable, and that required as little human interaction as was practically possible. We considered clinical applicability, the accuracy of segmentation, and processing time. The authors of the paper suggest using a Hidden Markov random field method in order to accurately segment the tumour from CT images in light of this information. The remaining parts of the paper are organised, such as previous works are discussed in section 2. The method that has been suggested is outlined in the third section. Section 4 contains the discussion of the experiment as well as the results of the experiment. The conclusion is broken down into its component parts and summarised in Section 5.

III. Proposed System

An HMRF model is regarded as the standard segmentation technique for images. In contrast, a preliminary estimate of brain tissue segmentation is required for the model. The brain's anatomy is both peculiar and intricate. The most fundamental obstacles in segmenting brain tissue are the volume effect and imaging artifacts such as noise and low-resolution imaging. Initial estimations with the HMRF model typically utilize a method of hard clustering. A complicated clustering approach makes sense for image segmentation when the image's boundaries are clearly defined. On the other hand, it is difficult to determine precisely where the brain image begins and ends. As a result, the technique known as hard clustering is unsuitable for the initial estimation.

Adaptive K-means clustering is used to estimate the brain tissue, followed by HMRF image segmentation to estimate the liver tissue. In our proposed model, both of these methods are utilized. Three components comprise the proposed method: preprocessing, clustering, and segmentation. To perform its function, the liver must function independently from the rest of the

body. During preprocessing, we will separate the tumor's edges and enhance them. Figure 3.1 illustrates the procedure visually.

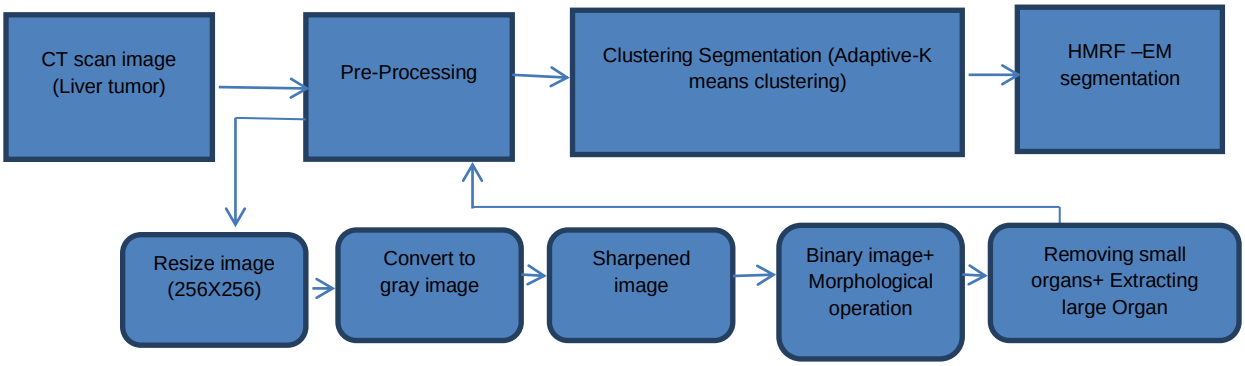

Fig. 3.1: Block Diagram of Proposed Method

The input image is obtained from the CT scan images. Those images were subjected to pre-processing.

3.1. Pre-processing

The proposed segmentation method necessitates a preprocessing phase to prepare the data for the segmentation procedure. To reduce the calculation's complexity, the input image is resized to a range of 250 by 250 pixels. If the image is represented in RGB format, it must be converted to grayscale. The sharpening of an image enhances its edges and fine details. After converting the image to binary format. The objective of a morphological operation is to eliminate image structure flaws. The majority of these operations are a combination of two processes: dilation and erosion. A structuring element is a small matrix structure utilized by the operation. The shape and size of the structural element substantially affect the final outcome. Then, the tiny organs are removed, and the tumor-containing large organs are extracted. Then, we employ the adaptive k-means algorithm, which optimizes the liver image and is usable by Hidden Markov Random Field (HMRF-EM).

3.2. Adaptive K-means Clustering

The adaptive K-means clustering algorithm begins with selecting K elements from the input data set via a randomization process in the first step. The K elements will serve as the seeds for the cluster, and a random selection process will be used to choose which ones to use. The characteristics of each component also serve as the characteristics of the cluster that the component in question is a part of, which means that each component's characteristics constitute the cluster's characteristics. Applying the algorithm allows one to calculate the distance between a particular element and a cluster. In addition to that, you can use this function to calculate the distance that exists between two distinct components by using the distance between them. This function needs to consider the distance based on the normalized properties of the objects. This is necessary to ensure that a single property does not dominate the distance or that some property is not ignored in the distance computation. Likewise, this is required to ensure that no property is overlooked in the distance calculation. The Euclidean distance will probably be sufficient for the majority of situations. For instance, in the case of n-dimensional spectral data, the distance separating any two data elements is n. E1 = {E11, E12,..., E1n} and E2 = {E21, E22,..., E2n} is given by $\sqrt{(E11 - E12)\,2 + (E12 - E22)\,2 + \cdots + (E1n - E2n)\,^2}$

It is essential to be aware that the square root function might be removed at some point in the near or distant future to achieve higher performance levels. The distance function may need to be modified in order to accommodate certain conditions. The first type of situation includes data in which one dimension is scaled differently than other dimensions, and the second type of situation includes data in which properties may be required to have different weights during the comparison. Two examples of each type of situation are provided in the following. The algorithm operates in the following manner when the distance function is being used: Determine the distance that separates each cluster from the others. Calculate the amount of space that separates each cluster. For future reference, a triangular matrix representing this distance has been stored in a two-dimensional array. In addition to this, we determine the two clusters that are the most closely related to one another and record the minimum distance, or dmin, that exists between any two clusters, such as Cm1 and Cm2. This allows us to determine which two clusters are the most closely related to one another. Determine the length of the distance that lies between each element Ei that is not a part of a cluster and the clusters themselves. When considering whether or not to include this component in a cluster, three distinct cases could come into play:

1. If the distance between an element and a cluster is 0, that element ought to be assigned to that cluster, and you ought to move on to the next element in the process if the distance remains 0 otherwise.
2. If the distance between the element and the cluster is less than the minimum distance, which is represented by the symbol dmin, then the element should be assigned to the cluster that is located the closest to it. It is possible that the cluster representation, which is also referred to as the centroid, will differ as a result of this assignment. The new method of computing the centroid takes the characteristics of all of the components that make up the cluster and uses them to determine an average value. In addition to this, we recalculate the distance that separates the affected cluster from every other cluster, the minimum distance between any two clusters, and the distance that exists between the two clusters that are situated in the closest proximity to one another.
3. The third and final scenario takes place when the distance dmin is less than the element's distance from the cluster that is physically closest to it. In this particular instance, we take the two clusters Cm1 and Cm2 that are located the most closely to one another geographically and combine them into a single cluster that we will refer to as Cm1.

In addition to this, we get rid of the cluster Cm2 by first removing all of the elements that make up that cluster, and then erasing any representation of the cluster that was there. After that, we place the new component into the cluster, which at this point is devoid of any members, effectively resulting in the formation of a new cluster. The distances that separate each of the clusters are recalculated, and the two clusters that were determined to be the ones that were physically closest to one another are identified again. The three procedures that were just outlined are repeated until all of the components have been categorized into their appropriate categories. In the event that some elements are situated at a considerable distance from other elements, there is a possibility that the algorithm will identify several singletons or clusters consisting of a single element in each of those instances. These are known as "outliers," and one way to find them is to look for clusters that have an unusually high. Searching for clusters with a minimal number of components can help identify outliers, which are components that should not be included in the clustering process. The alternative is to treat these elements as exceptions.

3.3. Hidden Markov Random Field Model

The HMRF is a method that can be used in practise for the segmentation of contextual images. The following is a mathematical explanation of the features that distinguish an HMRF model from others:

A. Markov Random Field

Let there be a random field in the infinite state space L denoted by X=X i,iS. The probability distribution can be expressed in the following way.

$$P(x) = Z^{-1}\exp(-U(x)) \quad (1)$$

S ={1,2,.. *N*} is the set of indices. The state *X* is not observable.

B. Observable Random Field

Let there be a random field in the infinite state space D denoted by Y = Yi, iS. Every Yi in a particular configuration xX conforms to a conditional probability distribution that is already known as P(y i |x i). The term for this type of function is the emission distribution probability function. Y represents the random field that is being emitted here.

C. Conditional Independence

For any $x \epsilon X$, the random variables *Yi* are conditionally independent.

$$P(y|x) = \prod_{i\in s} P(y_i|x_i) \quad (2)$$

Now the joint probability of any pair of (*Xi, Yi*) with the neighborhood of *Xi* is represented as:

$$P(y_i x_i|x_{Ni}) = P(y_i|x_i)\, P(x_i|x_{Ni}) \quad (3)$$

Where *Ni x* is the neighborhood configuration of *xi*. Now, the marginal probability distribution of *Yi* is computed depending on the parameter set and the neighborhood configuration.

$$P(Y_i|X_{Ni},\theta) = \sum_{l\in L} P(Y_i, l|X_{Ni},\theta) \quad (4)$$

Where $\theta = \{\theta_i, i \in L\}\{,\}$ is the parameter set.

The spatial dependence of the HMRF model is represented by the equation presented above. As a result, the HMRF model offers a model that is more adaptable for modelling images and encoding the statistical and spatial properties. Let there be a pixel known as x I j), whose local first-order neighbourhood E(y) is the collection of other pixels that have the positions I and j.

(*i, j+1*), (*i, j-1*), (*i-1, j*), (*i+1, j*). Then, the conditional density takes the form as,

$$E(y) = \frac{1}{\sqrt{2\pi}}\exp[-\frac{1}{2}x_{i,j} - \frac{1}{4}(x_{i,j+1} + x_{i-1,j} + x_{i+1,j})^2] \quad (5)$$

The HMRF model makes use of a number of different cliques. A clique is a collection of pixels that are in close proximity to one another and share the same colour. The order of a clique is determined by the individual pixels that make up the clique. The conditional probability density of the clique, which takes into account its surroundings, is used to compute the clique energy. The expression for the energy function is as follows:

$$U(y) = [\frac{1}{2}\ln(\sigma_t^2 + \frac{(x-\mu_t)^2}{2\sigma_t^2})] + E(y) \quad (6)$$

Two parts make up the representation of the energy function (6). The energy of the surrounding neighbourhood as well as the binding of the clusters in the image. The total energy of a label field is denoted by the symbol U(y) in this context. Both the initial mean vector and the initial covariance vector of segment t are denoted by the notation t, which stands for "t."

IV. Result and Discussion

A proposed method for segmentation based on elapsed time is examined in this section. Our illustration of input and output images is shown in figure 4.1. For liver tumor segmentation, we use CT images. It is first resized and sharpened before being transformed into a binary image.

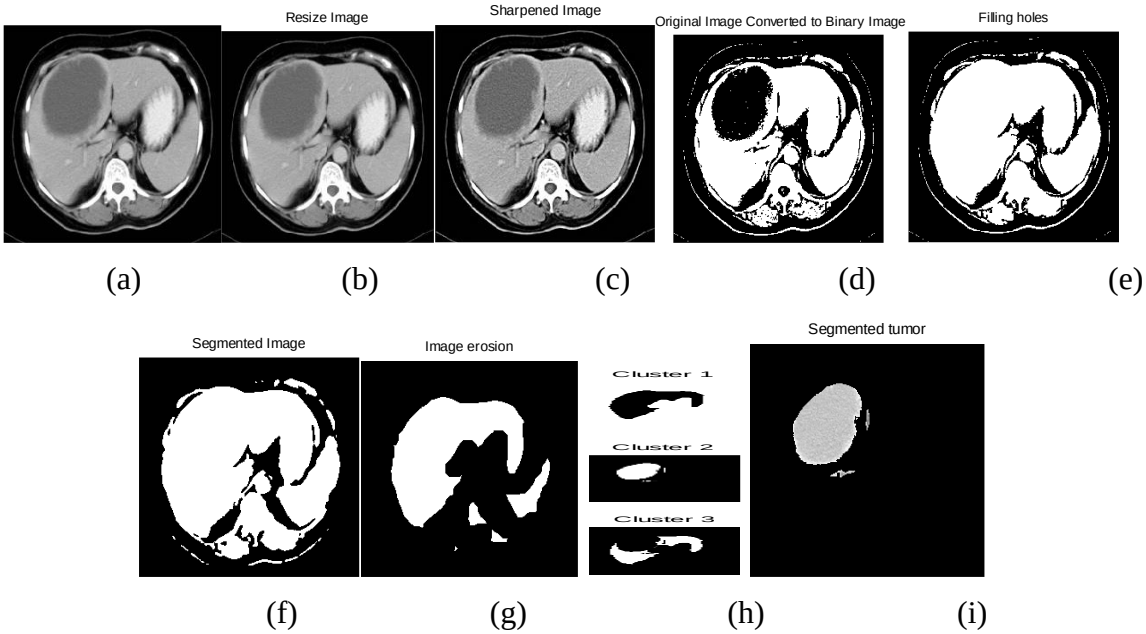

Fig. 4.1: Segmented Results. (a) Input Liver Image, (b) Resize Image, (c) Sharpened Image, (d) Binary Image, (e) Filling Holes, (f) Segmented Image, (g) Image Erosion, (h) Clustering, (i) Segmented Tumor.

In the subsequent step, we will carry out the morphological operation, during which we will open and close the morpheme and then fill it with the content that we require. After the image has been segmented and eroded, the cancerous growth can be seen plainly. After the image has been clustered, high-resolution microfocus radiation field electron microscopy (HMRF-EM) is used to precisely separate the tumor from the tissue that surrounds it.

Table 4.1: Result Comparison

No. of Training Images	**Elapsed time(sec)**	
	Existing Fuzzy K-C-Means Segmentation	**HMRF-EM**
Image 1	21.5585	1.576895
Image 2	19.3652	1.771440
Image 3	17.9856	1.718464
Image 4	19.2354	1.673772
Image 5	19.5961	1.805676

Compared to the existing fuzzy c mean clustering method, the segmentation process using the HMRF-EM method takes significantly less time and involves fewer iterations. As a result, the accuracy of the proposed method is superior to that of the system currently in place, which is illustrated in table 4.1.

V. Conculsion

Segmenting liver CT images has never been easier thanks to our new, fully automated method. HMRF-EM is the method's skeleton and foundation. The HMRF model and MRF-MAP estimation are combined with the EM fitting procedures. The HMRF-EM algorithm and the Adaptive k-means clustering algorithm were combined. The system keeps track of how much time has passed since the segmentation process began. With this model, we have found that it is possible to create a hidden random field, where the hidden random field is composed of continuous vectors, and the observed random field is the one that corresponds to the image. Here is where you can find this model. Two random fields can communicate with each other using the HMRF distribution. Results in table 1 show that the proposed system takes much less time than the fuzzy c-means algorithm to perform the same task. As a result, the proposed system's accuracy is superior to that of the current system. The algorithm has been put through its paces on various images, and the results have been impressive.

References

[1] Forner A, Llovet JM, Bruix J. Hepatocellular carcinoma. The Lancet. 2012; 379(9822): 1245-1255.

[2] Cornelis F, Martin M, Saut O, Buy X, Kind M, Palussiere J, et al. Precision of manual two-dimensional segmentations of lung and liver metastases and its impact on tumour response assessment using RECIST.

[3] Oliver, J.H. & Baron, R.L. Helical biphasic contrast-enhanced ct of the liver: technique, indications, interpretation, and pitfalls. Radiol. 201, 1–14 (1996).

[4] Stawiaski, J., Decencire, E., Bidault, F. Interactive liver tumor segmentation using graph cuts and watershed. In: Workshop on 3D Segmentation in the Clinic: A Grand Challenge II. Liver Tumor Segmentation Challenge. MICCAI (2008). ttp://hdl.han dle.net/10380/1416

[5] Lu, R., Marziliano, P., Thng, C.: Liver tumor volume estimation by semi-automatic segmentation method. In: Proceedings of the 27th Annual International Conference of the Engineering in Medicine and Biology Society, pp. 3296–3299 (2005). doi: 10.1109/IEMBS.2005.1617181

[6] Yim, P., Foran, D.: Volumetry of hepatic metastases in computed tomography using the watershed and active contour algorithms. In: Computer-Based Medical Systems, 2003. Proceedings. 16th IEEE Symposium, pp. 329–335 (2003). doi:10.1109/CBMS. 2003.1212810

[7] Li, B.N., Chui, C.K., Chang, S., Ong, S.H. A new unified level set method for semi-automatic liver tumor segmentation on contrast-enhanced CT images. Expert Syst. Appl., 39(10), 9661–9668 (2012).
doi:10.1016/j.eswa.2012.02.095

[8] Smeets, D., Loeckx, D., Stijnen, B., Dobbelaer, B.D., Vandermeulen, D., Suetens, P. Semi-automatic level set segmentation of liver tumors combining a spiral-scanning technique with supervised fuzzy pixel classification. Med. Image Anal., 14(1), 13–20 (2010).
doi:10.1016/j.media.2009.09.002

[9] Wong, D., Liu, J., Yin, F., Tian, Q., Xiong, W., Zhou, J., Yingyi, Q., Han, T., Venkatesh, S., Wang, S.: A semi-automated method for liver tumor segmentation based on 2D region

growing with knowledge-based constraints. In: Medical Image Computing and Computer Assisted Intervention (2008).
http://hdl.handle.net/ 10380/1428

[10] Zhou, J.Y., Wong, D.W.K., Ding, F., Venkatesh, S.K., Tian, Q., Qi, Y.Y., Xiong, W., Liu, J.J., Leow, W.K. Liver tumour segmentation using contrast-enhanced multi-detector CT data: performance benchmarking of three semiautomated methods. Comput. Appl. Eur. Radiol., 20(7), 1738–1748 (2010).

[11] Freiman, M., Eliassaf, O., Taieb, Y., Joskowicz, L., Azraq, Y., Sosna, J.: An iterative Bayesian approach for nearly automatic liver segmentation: algorithm and validation. Int. J. Comput. Assist. Radiol. Surg., 3(5), 439–446 (2008). doi:10.1007/s11548-008-0254-1

[12] Zhou, J., Xiong, W., Tian, Q., Qi, Y., Liu, J., Leow, W.K., Han, T., Venkatesh, S.K., Wang, S. Semi-automatic segmentation of 3D liver tumors from CT scans using voxel classification and propagational learning. In: Workshop on 3D Segmentation in the Clinic: A Grand Challenge II Liver Tumor Segmentation Challenge (2008).

[13] Moltz, J., Bornemann, L., Dicken, V., Peitgen, H.: Segmentation of liver metastases in CT scans by adaptive thresholding and morphological processing. In: Workshop on 3D Segmentation in the Clinic: A Grand Challenge II Liver Tumor Segmentation Challenge (2008). http://hdl.handle.net/10380/1419

[14] A.M. Anter, M.A. ElSoud, A.E. Hassanien et al., "Automatic computer aided segmentation for liver and hepatic lesions using hybrid segmentations techniques," In Proceedings of the 2013 Federated Conference on Computer Science and Information Systems, pp. 193–198, 2013.

[15] J.Y. Zhou, D.W.K. Wong, F. Ding et al., "Liver tumour segmentation using contrast-enhanced multi-detector CT data: Performance benchmarking of three semiautomated methods," European Radiology, vol. 20, no. 7, pp. 1738–1748, 2010.

[16] S.S. Kumar, R.S. Moni, and J. Rajeesh, "Contourlet transform based computer-aided diagnosis system for liver tumors on computed tomography images," In Proceedings of the 2011 - International Conference on Signal Processing, Communication, Computing and Networking Technologies, ICSCCN-2011, pp. 217– 222, ind, July 2011.

[17] M. Moghbel, S. Mashohor, R. Mahmud, and M. Iqbal Bin Saripan, "Automatic liver tumor segmentation on computed tomography for patient treatment planning and monitoring," EXCLI Journal, vol. 15, pp. 406–423, 2016.

[18] A. Das and S.K. Sabut, "Kernelized Fuzzy C-means Clustering with Adaptive Thresholding for Segmenting Liver Tumors," In Proceedings of the 2nd International Conference on Intelligent Computing, Communication and Convergence, ICCC 2016, pp. 389–395, January 2016.

[19] B.N. Li, C.K. Chui, S. Chang, and S.H. Ong, "A new unified level set method for semi-automatic liver tumor segmentation on contrast-enhanced CT images," Expert Systems with Applications, vol. 39, no. 10, pp. 9661–9668, 2012.

[20] T.N. Le, P.T. Bao, and H.T. Huynh, "Liver Tumor Segmentation from MR Images Using 3D Fast Marching Algorithm and Single Hidden Layer Feedforward Neural Network," BioMed Research International, vol. 2016, Article ID 3219068, 2016.

[21] J. Stawiaski, E. Decenciere, and F. Bidault, "Interactive liver tumor segmentation using graph-cuts and watershed," The MIDAS Journal - Grand Challenge Liver Tumor Segmentation (MICCAI Workshop), pp. 1–12, 2008.

[22] M.G. Linguraru, W.J. Richbourg, J. Liu et al., "Tumor burden analysis on computed tomography by automated liver and tumor segmentation," IEEE Transactions on Medical Imaging, vol. 31, no. 10, pp. 1965–1976, 2012.

[23] X. Zhang, J. Tian, D. Xiang, X. Li, and K. Deng, "Interactive liver tumor segmentation from ct scans using support vector classification with watershed," in Proceedings of the 33rd Annual International Conference of the IEEE Engineering in Medicine and Biology Society, EMBS 2011, pp. 6005–6008, usa, September 2011.

[24] S. Kadoury, E. Vorontsov, and A. Tang, "Metastatic liver tumour segmentation from discriminant Grassmannian manifolds," Physics in Medicine and Biology, vol. 60, no. 16, pp. 6459–6478, 2015.

[25] A.H. Foruzan and Y.W. Chen, "Improved segmentation of low-contrast lesions using sigmoid edge model," International Journal of Computer Assisted Radiology and Surgery, vol. 11, no. 7, pp. 1267–1283, 2016.

[26] X. Deng and G. Du, "Editorial: 3D segmentation in the clinic: a grand challenge II-liver tumor segmentation," The MIDAS Journal - Grand Challenge Liver Tumor Segmentation (MICCAI Workshop), pp. 1–4, 2008.